Analyst

Accepted Manuscript

ROYAL SOCIETY OF CHEMISTRY

www.rsc.org/analyst

Simultaneous Measurement and Quantitation of 4-Hydroxyphenylacetic acid and Dopamine with Fast-Scan Cyclic Voltammetry

Mimi Shin[1], Sam V. Kaplan[1], Kayla D. Raider[1], and Michael A. Johnson[1,2]

[1]Department of Chemistry and R.N. Adams Institute for Bioanalytical Chemistry, University of Kansas, Lawrence, KS 66045 USA
[2]Graduate Program in Neuroscience, University of Kansas, Lawrence, KS 66045 USA

*To whom correspondence should be addressed:
Prof. Michael A. Johnson
Department of Chemistry
Malott Hall, Room 2010
1251 Wescoe Hall Drive
Lawrence, KS 66045

Email: johnsonm@ku.edu
Phone: 785-864-4269

Abstract

Caged compounds have been used extensively to investigate neuronal function in a variety of preparations, including cell culture, *ex vivo* tissue samples, and *in vivo*. As a first step toward electrochemically measuring the extent of caged compound photoactivation while also measuring the release of the catecholamine neurotransmitter, dopamine, fast-scan cyclic voltammetry at carbon-fiber microelectrodes (FSCV) was used to electrochemically characterize 4-hydroxyphenylacetic acid (4HPAA) in the absence and presence of dopamine. 4HPAA is a by-product formed during the process of photoactivation of p-hydroxyphenylacyl-based caged compounds, such as p-hydroxyphenylglutamate (pHP-Glu). Our data suggest that the oxidation of 4HPAA occurs through the formation of a conjugated species. Moreover, we found that a triangular waveform of -0.4 V to +1.3 V to -0.4 V at 600 V/s, repeated every 100 ms, provided an oxidation current of 4HPAA that was enhanced with a limit of detection of 100 nM, while also allowing the detection and quantitation of dopamine within the same scan. Along with quantifying 4HPAA in biological preparations, the results from this work will allow the electrochemical measurement of photoactivation reactions that generate 4HPAA as a by-product as well as provide a framework for measuring the photorelease of electroactive by-products from caged compounds that incorporate other chromophores.

Introduction

The small molecule, 4-hydroxyphenylacetic acid (4HPAA), is a naturally occurring, electroactive phenolic compound formed in humans by the metabolism of aromatic amino acids.[1] Recent interest in phenolic compounds has centered on its propensity to become nitrated; thus, 4HPAA has been proposed to be a biomarker for certain disease conditions that result in an increase of nitrosative stress.[2] In addition, 4HPAA is used as a nutrient substrate in

microorganisms that metabolize it to pyruvate and succinate during the aerobic respiration.[3] More recently, 4HPAA has gained interest as an attenuator of DNA binding by Neisserial adhesin regulator (NadR) protein, a gene suppressor protein found in most hypervirulent strains of meningococcal bacteria.[4,5]

In addition to its biological functions, 4HPAA is a degradation product of the photoreaction of phenacyl-based caged compounds.[6–8] A caged compound possesses a photoactive trigger that inhibits the activity of its biological ligand; photoactivation, induced by exposure to light of the proper wavelength, results in the near-instantaneous release of the photocage and subsequent activation of the ligand. Caged compounds have frequently been employed in the study of brain function, both *ex vivo* and *in vivo*.[9–12]

The phenacyl-based photoreaction (Scheme 1, Supplementary Information) involves a Favorskii rearrangement, resulting in the formation of the activated biological molecule and 4HPAA. This reaction occurs, in some cases, within microseconds.[13] The quantitation of 4HPAA, therefore, provides an opportunity to indirectly quantify that amount of biologically active molecule formed by this reaction. Neurotransmitter molecules similar in structure to 4HPAA, such as tyramine and octopamine, have been shown to be electroactive and are readily detectable by fast-scan cyclic voltammetry (FSCV) at carbon-fiber microelectrodes. FSCV is a well-established electrochemical method that provides sub-second temporal resolution and good chemical selectivity when used for the detection of biogenic amine neurotransmitters.[14] Similarly, in this study, we have found that 4HPAA is also easily detectable by FSCV.

We have recently focused our efforts towards the sub-second quantitation of 4HPAA with the goal of quantitatively measuring the impact of caged compound photoactivation on dopamine (DA) release in brain tissue slices and *in vivo*. An important step in this process is the

electrochemical characterization and optimization of 4HPAA with FSCV. Our results suggest that 4HPAA undergoes an irreversible, two-electron oxidation that involves the formation of the conjugated species. Moreover, we have optimized the voltammetric waveform to enhance sensitivity to 4HPAA while also detecting DA simultaneously within the same scan. Using the optimized waveform, a limit of detection of 100 nM and a linear response up to 500 µm was found, indicating that FSCV could be used to detect 4HPAA in physiological fluid as well as quantify how much caged compound was photoreleased in the brain, both *in vivo* and *ex vivo*.

2. Experimental Procedures

2.1 Chemicals and solutions

DA, 4-hydroxyphenylacetic acid (4HPAA), and 4-methoxyphenylacetic acid (4MPAA) were purchased from Sigma-Aldrich (St. Louis, MO, USA). Methyl-4-hydroxyphenyl acetate (M4HPA) was acquired from Alfa Aesar (Ward Hill, MA). All aqueous solutions were made with purified (18.2 MΩ) water. Flow cell injection experiments were carried out in artificial cerebrospinal fluid (aCSF) or phosphate buffer as specified. The aCSF consisted of 126 mM NaCl, 2.5 mM KCl, 1.2 mM NaH_2PO_4, 2.4 mM $CaCl_2$, 1.2 mM $MgCl_2$, 25 mM $NaHCO_3$, and 20mM HEPES, and the pH was adjusted to 7.4. The phosphate buffer consisted of 3.3 mM KH_2PO_4 and 5.8 mM $NaH_2PO_4 \cdot 2H_2O$, and the pH was adjusted to 2.71, 6.71, and 10.71 respectively. Concentrated stock solutions were prepared in 0.2 M perchloric acid and were diluted with appropriate buffer for each experiment to desired concentrations on the beginning day of each experiment.

2.2 Carbon-Fiber Microelectrode Fabrication

Cylindrical carbon-fiber microelectrodes were fabricated as previously described.[15] Briefly, a 7 µm diameter carbon-fiber (Goodfellow Cambridge LTD., Huntingdon, UK) was loaded into a

glass capillary tube (1.2 mm O.D and 0.68 mm I.D, 4 in long; A-M system Inc, Carlsborg, WA, USA), which was then pulled using a PE-22 heated coil puller (Narishige Int. USA, East Meadow, NY). Next, the carbon fiber was trimmed to about 30 μm from the pulled glass tip, which was sealed with epoxy resin (EPON resin 815C, EPIKURE 3234 curing agent, Miller-Stephenson, Danbury, CT, USA) and cured at 100 °C for 1 hour. The electrodes were backfilled with 0.5 M potassium acetate to obtain an electrical connection between the carbon-fiber and electrode holder. Prior to the experiment, all electrodes were soaked in isopropanol for 10 minutes, and then electrochemically pretreated by scanning with the appropriate waveform, used for each experiment, at a frequency of 60 Hz for 15 min and 10 Hz for 10 min. A Ag/AgCl wire, locally fabricated, was used as the reference electrode.

2.3 Electrochemical Experiments

FSCV data were collected with a custom-modified ChemClamp potantiostat (Dagan, Minneapolis, MN, USA) and TarHeel CV software provided by R.M. Wightman and M.L.A.V. Heien (University of North Carolina, Chapel Hill, NC, USA). Measurements were acquired using a two-electrode electrochemical cell. For flow cell injection analysis, a six-port sample injector valve with 2 mL sample loop was mounted on a 2-position electric actuator (Valco Inc. Houston, TX, USA). As the actuator was triggered by the software, it rotated the valve to inject the sample for five seconds into a locally-constructed flow cell where the carbon-fiber working electrode and reference electrode were located. Cyclic voltammograms were collected every 100 ms. The scan rate and waveform potentials were varied as needed.

Conventional scan cyclic voltammetry was carried out using a 730E biopotentiostat (CH Instruments, Austin, TX) with a standard three-electrode system. A 3mm glassy carbon electrode was used as the working electrode, a platinum wire was used as the counter electrode, and a

Ag/AgCl electrode was used as the reference electrode (CH Instruments, Austin, TX). Prior to collecting measurements, the glassy carbon electrode was polished with an electrode polishing kit (CH Instruments, Austin, TX). For cyclic voltammetry experiments, 2mM 4HPAA was prepared in aCSF (pH 7.4) and then loaded into a locally constructed electrochemical cell. The potential was scanned from -0.4 V to either +1.0 V or +1.3 V, and the back to -0.4 V, at a scan rate of 10 mV/s. The glassy carbon electrode was re-polished between experiments, and the reference electrode was stored in 1M KCl while not in use. For data analysis, Electrochemical Analyzer software (CH Instruments, Austin, TX) was used.

2.4 Statistics

All numerical values were represented as mean ± standard error of the mean (SEM). For all analyses, n is equal to the number of electrodes. GraphPad Prism 6 (GraphPad Software Inc, La Jolla, CA, USA) was used to conduct statistical calculations and to present data.

3. Results and Discussion

3.1 Fast-Scan Cyclic Voltammetry of 4HPAA

The chemical structure of 4HPAA features a phenol group with an acetic acid group attached at the para position (Scheme 1A). For our initial detection of 4HPAA with FSCV, a standard triangular waveform, similar to that used to previously detect DA,[16] was applied to a carbon-fiber microelectrode by linearly scanning the electrode potential from –0.4 V to +1.0 V and back to –0.4 V at a scan rate of 400 V/s and an update rate of 10 CVs/s. The non-faradaic charging current was removed by subtraction of a set of averaged background scans collected from the same file. A representative CV is shown in Fig. 1A.

<Please insert scheme 1, single column size>

Scheme 1. Proposed oxidation reactions of 4HPAA, M4HPA, and 4MPAA. (A) Oxidation of 4HPAA to form a conjugated species and (B) the decarboxylation of 4HPAA. (C) Oxidation of methyl-4-hydroxyphenyl acetate (M4HPA) and (D) 4-methoxyphenylacetic acid (4MPAA).

The CVs obtained by FSCV were plotted in an unfolded manner, in which the switching potential is located at the center of the plot, in order to clarify the location of the oxidation peaks. The color plot and corresponding CV revealed that a large, faradaic current peak, due to the oxidation of 4HPAA, occurs at approximately + 0.9 V as the potential was being scanned from + 1.0 V to – 0.4 V. The occurrence of this peak on the reverse scan is atypical; current due to the oxidation of many electroactive neurotransmitters, such as (DA) and serotonin (5-HT), occur on the front, forward scan. On the other hand, the oxidation peak of hydrogen peroxide also occurs on the reverse scan under similar scan parameters.[17] Additionally, histamine and adenosine have oxidation peaks detected on the reverse scan , exhibiting similar electrochemical behavior to that of 4HPAA and hydrogen peroxide.[18,19] The authors stated that this phenomenon could have been caused by the time required for electron transfer. It should also be noted that the oxidation peak of 4HPAA occurred on the reverse scan even before filtering the file.

<Please insert figure 1 here, single column size>

A broad, shallow negative current (less than 10% of the oxidation current) also occurred on the forward scan. The cause of this peak is unclear; however, this particular peak does not appear on the first CV collected, but does appear on CVs collected 2 seconds after the electrode was exposed to a 4HPAA bolus (data not shown). Therefore, it is possible that the peak is caused by the formation and adsorption of a species as a result of the initial 4HPAA oxidation.[20]

However, it is not clear if this current is faradaic or if it occurs as a result of an alteration in the electrode background.

The current response at the oxidation potential of 4HPAA is shown in Fig 1B. This current trace (top) has a square response to a 4HPAA bolus during the sample injection analysis. Overall, the features of this CV, namely, the disparity in magnitude and the absence of a faradaic reduction peak on the reverse scan, suggest that 4HPAA undergoes an irreversible electrochemical reaction under these conditions.

3.2 Mechanisms of oxidation of 4HPAA

Two potential mechanisms that could be responsible for the oxidation current in Fig. 1 include the oxidation of 4HPAA to form a conjugated specie (Scheme 1A) and/or the decarboxylation of 4HPAA (Scheme 1B). The conjugated specie is formed by a two-electron oxidation reaction in which the phenolic proton and one of the protons located on the β-carbon are removed. On the other hand, the decarboxylation reaction occurs when one of the protons located on the negatively-charged carboxylic acid group is removed, forming a radical that results in the release of a carbon dioxide molecule.

<Please insert figure 2 here, double column size>

To examine these potential mechanisms, we obtained CVs of 4HPAA and the related compounds, methyl-4-hydroxyphenyl acetate (M4HPA) and 4-methoxyphenylacetic acid (4MPAA) (Schemes 1C and 1D, respectively) at pH values of 2.71, 6.71, and 10.71 (Fig. 2). The same electrochemical parameters employed in Fig.1 were used for these pH studies. At all pH values, 4HPAA and M4HPA showed substantial faradaic oxidation currents that occurred on the

reverse scan at about +0.9 V and +0.8 V, respectively, while 4MPAA showed no appreciable current at any pH. The pH value significantly impacted the oxidative current; responses progressively decreased for 4HPAA and M4HPA, with the highest current observed at pH 2.71 and the lowest current observed at pH 10.71 ($p < 0.0001$, n=4, two-way ANOVA, $F(2,90) = 56.94$).

The evidence presented here suggests that the oxidation of 4HPAA proceeds through the formation of conjugated species. The para-methoxy derivative form of 4HPAA, 4MPAA, showed only a negligible oxidation current compared to 4HPAA. This is not surprising, given that the methoxy group on the ring would be expected to make the formation of the conjugated specie energetically unfavorable. On the other hand, M4HPA showed an oxidation current similar to 4HPAA at all pH values. Given that both M4HPA and 4HPAA possess an oxidizable phenol group, both compounds can readily form the conjugated species (Scheme 1A and 1C). The idea that M4HPA and 4HPAA undergo similar oxidation mechanisms is supported by other reports in which the redox behavior of parabens and other analogues was investigated.[21] Gil et al. have employed an electrochemical method to investigate the association between the inductive effect of different types of parabens and their redox behavior.[21] This study suggests that the phenolic hydroxyl group affects the oxidation state of parabens; thus, changes in pH influence redox reactions, especially those involving H^+.

This overall trend of decreasing oxidation current with decreasing pH seems to be influenced by pH-induced charged states of 4HPAA and M4HPA. The pKa values of the phenolic carboxylic acid and hydroxyl group of 4HPAA are 4.48 and 9.67, respectively; thus, 4HPAA is neutral under highly acidic conditions and negatively charged under neutral and basic conditions.[22] However, the pKa value of M4HPA is 8.4, making M4HPA neutral under both

acidic and neutral conditions and negatively charged under highly basic conditions. When the waveform in Fig. 1 is employed, the surface of the carbon-fiber microelectrode is held at a potential of -0.4 V during the 93 ms that elapses in between 7 ms-duration voltage sweeps. This electron-rich state would be expected to promote adsorption of positively-charged species while repelling negatively-charged species. Our observations in Fig. 2 are consistent with this logic. The oxidation currents for both 4HPAA and M4HPA are lowest at a pH of 10.71, conditions under which both species are negatively charged, and are greatest at a pH of 2.71, at which both species are neutral in charge.

The currents arising from the oxidation of M4HPA are greater than those arising from 4HPAA oxidation at pH values of 6.71 and 10.71. This difference likely occurs because 4HPAA possesses a single negative charge compared to the neutral charge state of M4HPA at a pH of 6.71. Similarly, 4HPAA has a double negative charge while M4HPA has a single negative charge at a pH of 10.71. The increased negative character of 4HPAA would be expected to decrease its association with the negatively-charged electrode surface to a greater extent than M4HPA, thereby decreasing the measured oxidation currents of 4HPAA at neutral and basic pH.

In addition to altering the charge state of the molecules of interest, pH can also influence the carbon-fiber microelectrode surface. Oxide groups on the surface can undergo protonation and deprotonation as environmental pH changes, thereby affecting electrochemical responses.[23,24] Moreover, the changes in pH tend to influence redox reactions, especially those involving a loss or gain of H^+, as is commonly observed in phenolic compounds.[25] It is not clear if these modifications would differentially influence oxidation currents obtained from 4HPAA and M4HPA.

<Please insert figure 3 here, double column size>

Currents measured at the electrode may be controlled in two fundamental ways: (1) the electron transfer reaction of 4HPAA adsorbed onto the electrode surface cannot keep up with the high scan rates employed when using FSCV (electron transfer-limited current) and (2) the oxidation currents are limited by the ability of 4HPAA to diffuse to the electrode due to the high scan rates employed (diffusion-limited current). To determine if the current is adsorption- or diffusion-limited, we obtained CVs at scan rates ranging from 100 to 800 V/s (Fig. 3). When the current response was plotted against various scan rates, shown in Fig 3A, linear responses were observed up to 500 V/s (R^2=0.9882), suggesting that the electrochemical reaction is adsorption dependent up to this scan rate.[26] At scan rates greater than 500 V/s, linearity is lost; however, when these current responses were plotted versus square root of scan rate, as shown in Fig 3B, the plot yielded a linear trace (R^2 =*0.9822*), suggesting diffusion control.[16,27] Therefore, we conclude that electron transfer kinetics for 4HPAA oxidation are influenced mostly by adsorption at scan rates below 500 V/s, and diffusion at scan rates greater than 500 V/s.[18] These factors likely contribute to the movement of the peak from higher to lower potentials (Fig. 3C), that is, the electron transfer reaction shifts farther to the right of the switching potential of +1.0 V.

<Please insert figure 4 here, single columns size>

To determine if additional oxidation processes can be induced at higher potentials, the waveform was modified so that the potential was scanned up to +1.3 V, while the holding potential was still maintained at -0.4 V at 400 V/s (Fig. 4). The resulting CV revealed the formation of two individual oxidation peaks, indicating the occurrence of two distinct

electrochemical processes (Fig. 4A). The first and second peaks were observed at +1.2 V on the forward scan ('peak 1') and at +1.0 V on the reverse scan ('peak 2'), respectively. To understand the possible mechanism of these two oxidation peaks' formation, the current traces were analyzed. The current for peak 1 increased more rapidly upon 4HPAA injection compared to peak 2 (Fig 4B, top) and reached a steady state almost before the second oxidation peak had begun to form. These traces are consistent with a mechanism in which the primary oxidation reaction, resulting in peak 1, is followed by a secondary oxidation reaction, resulting in peak 2.

<Please, insert figure 5 here, single column size>

Further analysis of 4HPAA with conventional cyclic voltammetry was conducted for comparison. For this experiment, a three electrode system was used. The potential at a glassy carbon electrode, immersed in a solution of 2 mM 4HPAA in aCSF, was scanned from -0.4 V up to +1.0 V and back to -0.4 V at a scan rate of 10 mV/s (Fig. 5A). In contrast to the measurements obtained with FSCV, the oxidation peak was detected at +0.65 V on the forward scan. Moreover, when the electrode was scanned up to the higher switching potential of +1.3 V, the two oxidation peaks were observed on forward sweep, at +0.65 V and +1.06 V, as expected (Fig. 5B).

Although the electrochemical mechanism underlying the formation of this second peak is not clear, it is possible that a dimerization occurs. The phenol group of the 4HPAA molecule is reactive since the proton from the hydroxyl group is acidic. Therefore, as the oxidation potential is applied to the electrode, the first electron is transferred from the phenol to the electrode, forming a phenoxy radical that further couples with another 4HPAA molecule to electrochemically generate a dimer, similar to that occurring with other phenolic

compounds.[21,22,28–30] As the dimer forms, the second electron transfer takes place, which would be responsible for the second oxidation peak.[22]

During the collection of multiple CVs, the oxidation current of 4HPAA dropped substantially after the first scan, necessitating that the electrode must be polished between each scan (data not shown). With this in mind, it should be mentioned that poly-4HPAA can passivate the electrode surface, resulting in electrode fouling and slower electron transfer. Nevertheless, electrode fouling appeared not to substantially impact current from the FSCV experiments. One explanation for this is that the electrode was scanned at such a high rate that there is not enough time for electrodeposition to occur.[22]

3.3 Optimization of FSCV Scanning Parameters

To minimize the effect of the secondary product (peak 2) while enhancing the response of the main peak (peak 1), oxidation current responses of 4HPAA at different switching potentials, holding potentials, and scan rates were studied. First, we obtained CVs containing both main and secondary peaks at selected switching potentials ranging from +1.0 V to +1.4 V at the constant holding potential of -0.4 V and a scan rate of 400 V/s. Overall, the current response of peak 1 increased as the switching potential was changed from +1.0 V to +1.4 V (Fig 6A). A slight drop in current was found at +1.4 V. As higher switching potentials are applied, the hydrophobicity of the carbon-fiber electrode surface changes by increasing the number of oxide groups, which improves the electron transfer kinetics at the electrode surface and enhances sensitivity.[31,32] Such an improvement could also arise from an increase in the microscopic area of the electrode surface[33,34] and enhancement of hydrogen atom transfer, resulting in changing the charge at the electrode surface.[35,36]

<Please insert figure 6 here, double column size>

The current response due to the secondary reaction also increased with greater switching potential in the fast-scan CV traces, but not as much as the main peak. In fact, the current response of peak 1 was more than double that of peak two at +1.3 V. A similar effect has been well-documented when measuring DA.[37,38] Therefore, in order to optimize the ability of FSCV to measure DA, while also enhancing the 4HPAA signal, we selected +1.3 V as the switching potential.

Current response was measured at selected holding potentials (between -0.5V and +0.2V) while maintaining a switching potential at +1.3V at a scan rate of 400 V/s. (Fig. 6B). 4HPAA is negatively charged at the physiological pH, so we expected to see lower current responses for both peak 1 and peak 2 due to the repulsive action between the negatively charged electrode and 4HPAA conjugate base. However, a higher current response for peak 1 was observed as more negative holding potentials were applied except at -0.5 V, due to the unreliable background current at lower holding potentials.[18] This enhancement of catecholamine signal at negative holding potentials had previously been suggested to occur as a result of the increased amount of adsorption at the electrode surface.[16] The adsorption of 4HPAA apparently plays a major role, thereby explaining the current response increases that occur as the holding potential becomes more negative.

Increasing scan rate has also been shown to enhance the current response of adsorbed species (see Fig. 3).[39] Fig. 6C shows a plot of oxidation current of 4HPAA versus scan rate. As expected, the current for both peak 1 and peak 2 increased with scan rate. As faster scan rates are applied, the time spent at the holding potential increases, which also increases the amount of

time for adsorption as well. Even though the highest current is obtained at the scan rate of 800 V/s, we decided to use 600 V/s as an optimized parameter. This choice represents a compromise. At high scan rates, faradaic currents can be buried under the background current[37] which is proportional to the scan rate.[23] Moreover, DA, as well as other electroactive neurotransmitters, undergo hysteresis—the oxidation occurs at a more positive potential, the reduction occurs at a more negative potential—which may cause increased overlap with the 4HPAA peak.[16,40]

3.4 Cyclic Voltammetry of 4HPAA and DA

One of our goals is to be able to quantify how much 4HPAA has been photo-released from *p*-hydroxphenacyl-based caged compounds.[6,41] A specific application of this approach is the photorelease of glutamate, the most abundant excitatory neurotransmitter in the central nervous system,[42] in brain tissue and measuring subsequent alterations in the electrically evoked release of DA. This approach has the advantages of being able to apply glutamate within short timeframes and confined spatial dimensions. Both of these advantages are critical because glutamate is excitotoxic,[43] making the bath application of brain slices impractical. Unfortunately, determining with high precision the amount of glutamate, or any other caged compound that has been photoreleased, has historically relied upon experimental determination of the number of moles of photons per second supplied by the light source and multiplying this parameter by the quantum yield (moles of compound photoreleased/moles of photons supplied) of the caged compound of interest.[9] This method is inherently imprecise due to variations in the output of the light source as well inconsistencies in tissue density at various recording sites. One goal in the electrochemical characterization of 4HPAA is to use this electrochemical signature to quantify glutamate photorelease within brain tissue slices more reliably than the existing method

described, independent of the number of photons reaching the tissue. Therefore, it is important to optimize our voltammetric parameters for the simultaneous detection of DA and 4HPAA.

To enhance the peak separation, voltammetric measurements were obtained from a mixture of 4HPAA (100 μM) and DA (1 μM) at selected switching potentials while the holding potential was kept at -0.4 V (Fig 7A). As shown, the separation of peak oxidation potential (E_{ox}) between 4HPAA (100 μM) and DA (1 μM) was greatest at a switching potential of +1.3 V. The use of higher switching potentials is not well-suited for the detection of dynamic changes of catecholamine release due to the increased response time.[38] Therefore, we decided to use +1.3 V in the optimized waveform. Holding potential and scan rate did not significantly affect peak separation, so a potential of -0.4 V and rate of 600 V/s (the optimized scan rate for 4HPAA) was used.

<Please insert figure 7 here, double column size>

An example of the detection of 4HPAA and DA using this optimized waveform is shown in Figs. 7B and 7C. The oxidation peaks for both 4HPAA (peak 1) and DA rise rapidly after injection. Moreover, the peaks are clearly separated on the CV. The optimized waveform was used to measure the current signal of a mixture of 4HPAA and DA at selected concentrations (Fig. 7D). The current traces of both peak 1 and 2 have square responses due to the sample injection compared to that of DA, which shows a slower response under the same conditions. A similar difference in current response has been shown between DA and ascorbate. This is likely due to DA being strongly adsorbed and desorbed at the electrode surface.[16] For the data analysis on the calibration curve, the current was taken at the main oxidation peak of 4HPAA. Fig. 7 shows the oxidation current responses of the main peak as a function of 4HPAA concentration

which was varied from 0.1 μM to 100 μM in the presence of 1 μM DA in solution. The oxidation current of 4HPAA increases linearly with the concentration with correlation coefficient of 0.9905 up to 20 μM and 0.9701 up to 100 μM. The limit of detection of 4HPAA was found to be 100 nM based on the signal to noise ratio of 3.

Conclusions

The goal of this study was to develop a method to quantitatively and simultaneously measure sub-second changes in DA and 4HPAA levels. Our intent is to apply this method to examine neurotransmitter interactions in brain slices as well as *in vivo*. We found that the optimum waveform for the detection of 4HPAA was to scan linearly from a holding potential of -0.4 V to +1.3 V and back to -0.4 V at a scan rate of 600 V/s. This waveform provided good limits of detection and sensitivity for the measurement of 4HPAA. Moreover, this optimized waveform was effective for the simultaneous detection of 4HPAA and DA. Along with quantifying 4HPAA in biological preparations, the results from this work will allow the electrochemical measurement of photoactivation reactions that generate 4HPAA as a by-product as well as provide a framework for measuring the photorelease of electroactive by-products from caged compounds that incorporate other chromophores.

Acknowledgements

This work was financially supported by the National Institutes of Health (NIH 1R21NS077485) and University of Kansas COBRE Center for Molecular Analysis of Disease Pathways (NIH P20GM103638). The authors would like to thank Professor Dr. Richard Givens, University of Kansas, for suggestions regarding to the measurement of 4HPAA.

Graphic for Table of Contents

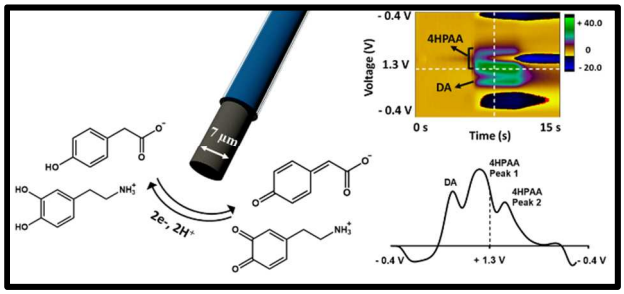

References

1. U. Takahama, T. Oniki and H. Murata, *FEBS Lett.*, 2002, **518**, 116–118.
2. H. Ischiropoulos, *Arch. Biochem. Biophys.*, 1998, **356**, 1–11.
3. W. A. Hareland, R. L. Crawford, P. J. Chapman and S. Dagley, *J. Bacteriol.*, 1975, **121**, 272–285.
4. M. M. E. Metruccio, E. Pigozzi, D. Roncarati, F. Berlanda Scorza, N. Norais, S. A. Hill, V. Scarlato and I. Delany, *PLoS Pathog.*, 2009, **5**, e1000710.
5. S. Brier, L. Fagnocchi, D. Donnarumma, M. Scarselli, R. Rappuoli, M. Nissum, I. Delany and N. Norais, *Biochemistry (Mosc.)*, 2012, **51**, 6738–6752.
6. R. S. Givens and J.-I. Lee, *J. Photoscience*, 2003, **10**, 37–48.
7. R. S. Givens, D. Heger, B. Hellrung, Y. Kamdzhilov, M. Mac, P. G. Conrad, E. Cope, J. I. Lee, J. F. Mata-Segreda, R. L. Schowen and J. Wirz, *J. Am. Chem. Soc.*, 2008, **130**, 3307–3309.
8. R. S. Givens, P. G. Conrad, A. L. Yousef, J. I. Lee, W. M. Horspool and F. Lenci, *CRC Press Boca Raton*, 2004.
9. G. C. R. Ellis-Davies, *Nat. Methods*, 2007, **4**, 619–628.
10. E. M. Callaway and L. C. Katz, *Proc. Natl. Acad. Sci.*, 1993, **90**, 7661–7665.
11. S. S.-H. Wang and G. J. Augustine, *Neuron*, 1995, **15**, 755–760.
12. J. M. Nerbonne, *Curr. Opin. Neurobiol.*, 1996, **6**, 379–386.
13. M. Goeldner and R. Givens, *Dynamic studies in biology: phototriggers, photoswitches and caged biomolecules*, Wiley-VCH, Weinheim, 2005.
14. S. E. Cooper and B. J. Venton, *Anal. Bioanal. Chem.*, 2009, **394**, 329–336.
15. M. A. Johnson, V. Rajan, C. E. Miller and R. M. Wightman, *J. Neurochem.*, 2006, **97**, 737–746.
16. B. D. Bath, D. J. Michael, B. J. Trafton, J. D. Joseph, P. L. Runnels and R. M. Wightman, *Anal. Chem.*, 2000, **72**, 5994–6002.
17. A. L. Sanford, S. W. Morton, K. L. Whitehouse, H. M. Oara, L. Z. Lugo-Morales, J. G. Roberts and L. A. Sombers, *Anal. Chem.*, 2010, **82**, 5205–5210.
18. B. K. Swamy and B. J. Venton, *Anal. Chem.*, 2007, **79**, 744–750.
19. S.-Y. Chang, T. Jay, J. Muñoz, I. Kim and K. H. Lee, *The Analyst*, 2012, **137**, 2158.
20. P. Takmakov, M. K. Zachek, R. B. Keithley, E. S. Bucher, G. S. McCarty and R. M. Wightman, *Anal. Chem.*, 2010, **82**, 9892–9900.
21. E. de S. Gil, C. H. Andrade, N. L. Barbosa, R. C. Braga and S. H. Serrano, *J. Braz. Chem. Soc.*, 2012, **23**, 565–572.

22. L. P. Rodrigues, D. C. Ferreira, M. T. Sonoda, A. G. B. Madurro, O. Abrahão and J. M. Madurro, *J. Mol. Struct.*, 2014, **1072**, 298–306.
23. P. Takmakov, M. K. Zachek, R. B. Keithley, P. L. Walsh, C. Donley, G. S. McCarty and R. M. Wightman, *Anal. Chem.*, 2010, **82**, 2020–2028.
24. P. L. Runnels, J. D. Joseph, M. J. Logman and R. M. Wightman, *Anal. Chem.*, 1999, **71**, 2782–2789.
25. G. Arslan, B. Yazici and M. Erbil, *J. Hazard. Mater.*, 2005, **124**, 37–43.
26. A. J. Bard and L. R. Faulkner, *Electrochemical methods: fundamentals and applications*, Wiley New York, 1980, vol. 2.
27. U. Chandra, B. K. Swamy, O. Gilbert, S. S. Shankar, K. R. Mahanthesha and B. S. Sherigara, *Int. J. Electrochem. Sci.*, 2010, **5**, 1–9.
28. C. M. de Castro, S. N. Vieira, R. A. Gonçalves, A. G. Brito-Madurro and J. M. Madurro, *J. Mater. Sci.*, 2008, **43**, 475–482.
29. A. M. Tenreiro, C. Nabais, J. P. Correia, F. M. S. S. Fernandes, J. R. Romero and L. M. Abrantes, *J. Solid State Electrochem.*, 2007, **11**, 1059–1069.
30. M. Ferreira, H. Varela, R. M. Torresi and G. Tremiliosi-Filho, *Electrochimica Acta*, 2006, **52**, 434–442.
31. M. R. Deakin, P. M. Kovach, K. J. Stutts and R. M. Wightman, *Anal. Chem.*, 1986, **58**, 1474–1480.
32. Z. R. Yue, W. Jiang, L. Wang, S. D. Gardner and C. U. Pittman Jr, *Carbon*, 1999, **37**, 1785–1796.
33. R. M. Wightman, M. R. Deakin, P. M. Kovach, W. G. Kuhr and K. J. Stutts, *J. Electrochem. Soc.*, 1984, **131**, 1578–1583.
34. K. J. Stutts, P. M. Kovach, W. G. Kuhr and R. M. Wightman, *Anal. Chem.*, 1983, **55**, 1632–1634.
35. G. N. Kamau, W. S. Willis and J. F. Rusling, *Anal. Chem.*, 1985, **57**, 545–551.
36. M. R. Deakin, K. J. Stutts and R. M. Wightman, *J. Electroanal. Chem. Interfacial Electrochem.*, 1985, **182**, 113–122.
37. R. B. Keithley, P. Takmakov, E. S. Bucher, A. M. Belle, C. A. Owesson-White, J. Park and R. M. Wightman, *Anal. Chem.*, 2011, **83**, 3563–3571.
38. M. L. A. V. Heien, P. E. M. Phillips, G. D. Stuber, A. T. Seipel and R. M. Wightman, *The Analyst*, 2003, **128**, 1413.
39. P. Kissinger and W. R. Heineman, *Laboratory Techniques in Electroanalytical Chemistry, revised and expanded*, CRC press, 1996.
40. C. Hsueh, R. Bravo, A. J. Jaramillo and A. Brajter-Toth, *Anal. Chim. Acta*, 1997, **349**, 67–76.
41. R. S. Givens, M. Rubina and J. Wirz, *Photochem. Photobiol. Sci.*, 2012, **11**, 472.
42. J. Cooper, F. Bloom and R. Roth, *Biomed. Pharmacother.*, 1997, **51**, 409–409.
43. L. P. Mark, R. W. Prost, J. L. Ulmer, M. M. Smith, D. L. Daniels, J. M. Strottmann, W. D. Brown and L. Hacein-Bey, *Am. J. Neuroradiol.*, 2001, **22**, 1813–1824.

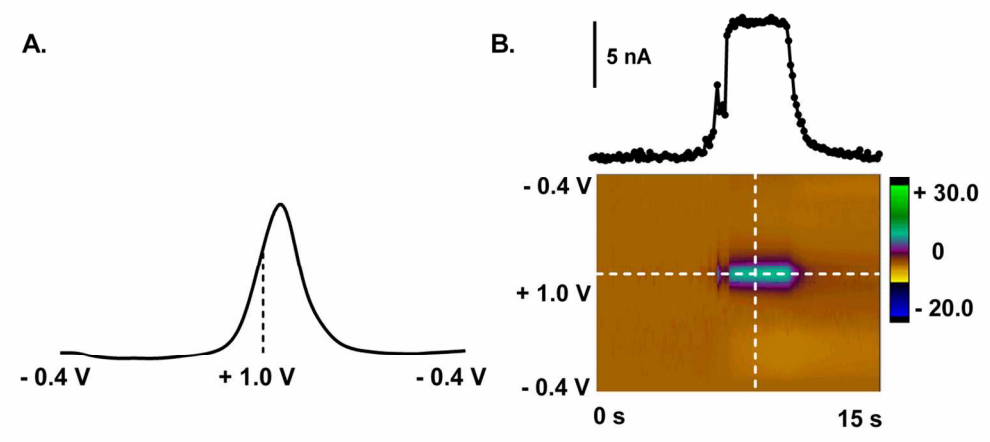

Fig. 1 Background subtracted cyclic voltammetry of 4HPAA. (A) Unfolded cyclic voltammogram of 100 μM of 4HPAA in aCSF, physiological pH 7.4, obtained using the waveform -0.4 V to +1.0 V to -0.4 V at 400 V/s every 100 ms. The oxidation peak of 4HPAA was detected around + 0.9 V on the reverse scan . (B) The color plot (bottom) and oxidation current response (top), taken at the oxidation peak of 4HPAA, were acquired as the carbon-fiber electrode was exposed to 4HPAA bolus for 5s during the flow injection analysis.
122x54mm (300 x 300 DPI)

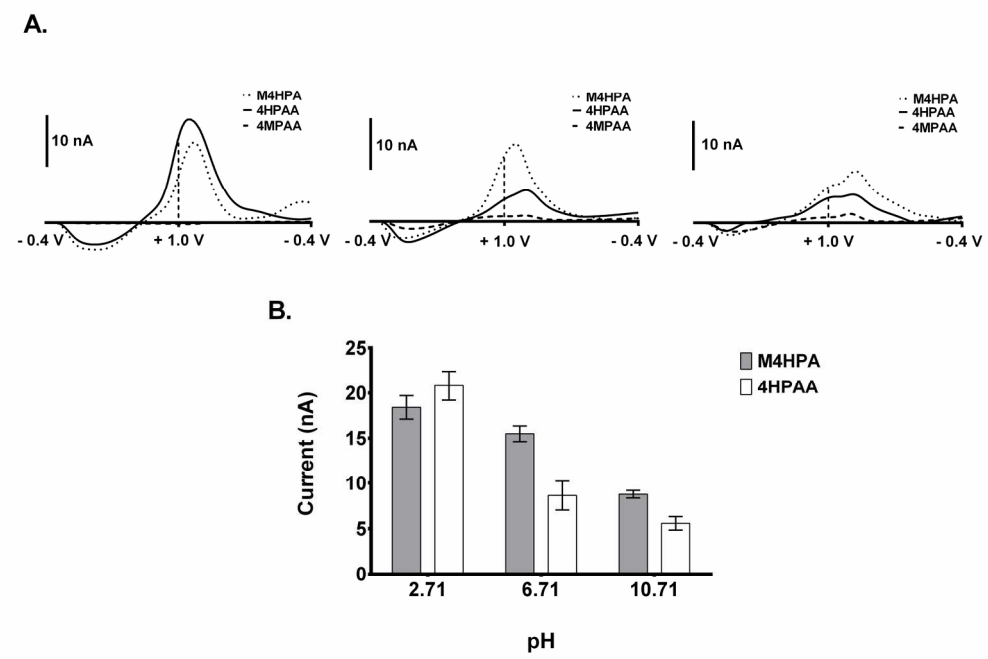

Fig. 2. Changes in oxidation signal of 4HPAA and M4HPA in response to pH. (A) Unfolded fast-scan CVs of 4HPAA and M4HPA at pH values of 2.71 (left), 6.71 (center), and 10.71(right). Oxidation peaks of both species were detected on the reverse scan. (B) The effect of pH on oxidation current of 4HPAA and M4HPA. Both species showed similar overall current trends in response to changes in pH. There was a significant pH-driven effect on oxidation current ($p = 0.0007$, $n=4$, two-way ANOVA, $F(2,90) = 56.94$)
189x128mm (300 x 300 DPI)

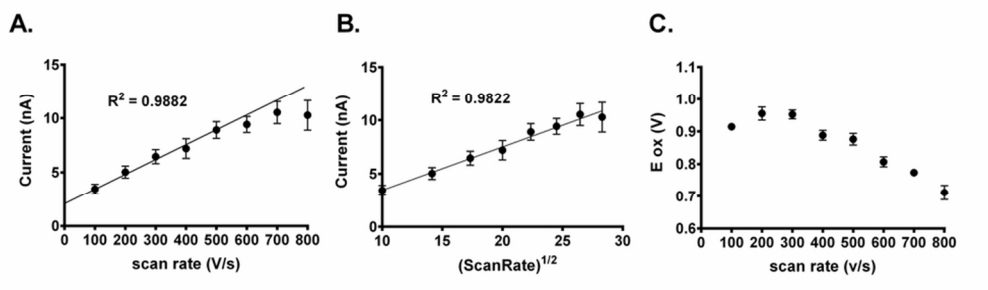

Fig. 3 The effect of scan rate on currents generated from the oxidation of 4HPAA. (A) Plot of current versus scan rate. The R^2 value applies to measurements obtained from 100 to 500 V/s. (B) Plot of current versus the square root of the scan rate. CVs were obtained using the waveform −0.4 V to +1.0 V to -0.4 V at selected scan rates. The currents were obtained from the oxidation peaks. (C) Plot of oxidation potential (E_{ox}) versus scan rate.
83x24mm (300 x 300 DPI)

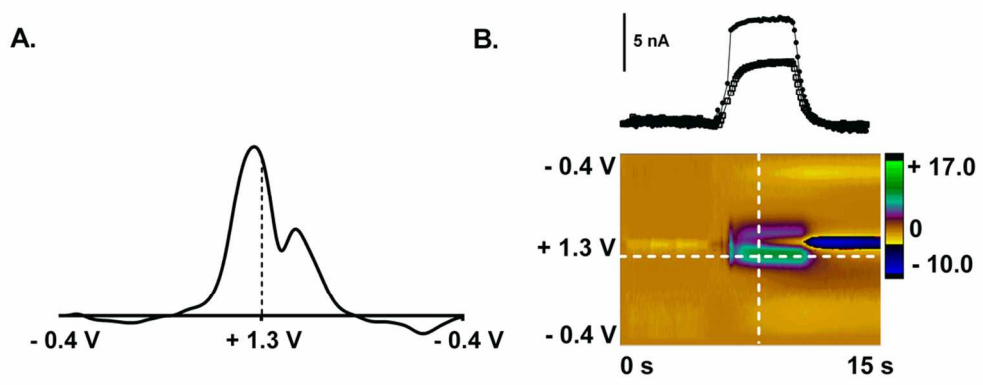

Fig. 4 Fast-scan cyclic voltammetry of 4HPAA. (A) Unfolded cyclic voltammogram of 100 µM 4HPAA in aCSF (pH 7.4) obtained using the waveform -0.4 V to + 1.3 V to -0.4 V at 400 V/s repeated every 100 ms. Two oxidation peaks were observed, one around + 1.2 V on the forward scan and the other one around +1.0 V on the reverse scan. (B) Color plot (bottom) and current traces taken at the first oxidation peak, observed on the forward scan.
103x41mm (300 x 300 DPI)

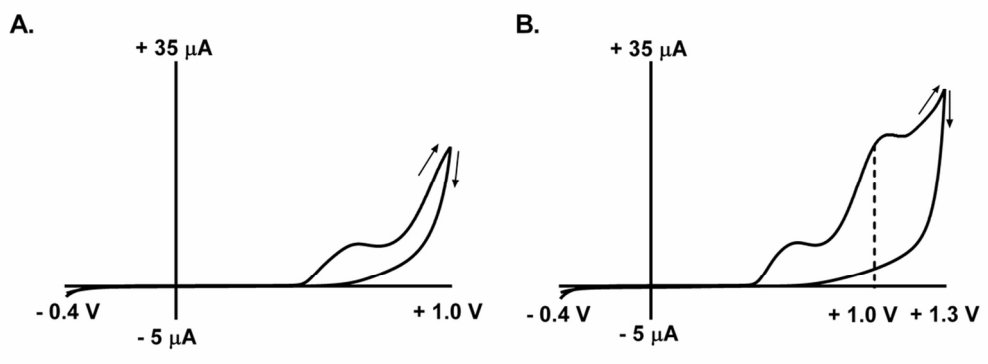

Fig.5 Conventional cyclic voltammetry of 4HPAA. (A) CV obtained using the waveform -0.4 V to +1.0 V to -0.4 V showing a single faradaic peak. (B) CV obtained using the waveform -0.4 V to +1.3 V to -0.4 V showing the appearance of an additional peak at +1.06 V. The dashed line denotes the location of the +1.0 V potential. The concentration of 4HPAA was 2 mM and the scan rate was 10 mV/s.
102x37mm (300 x 300 DPI)

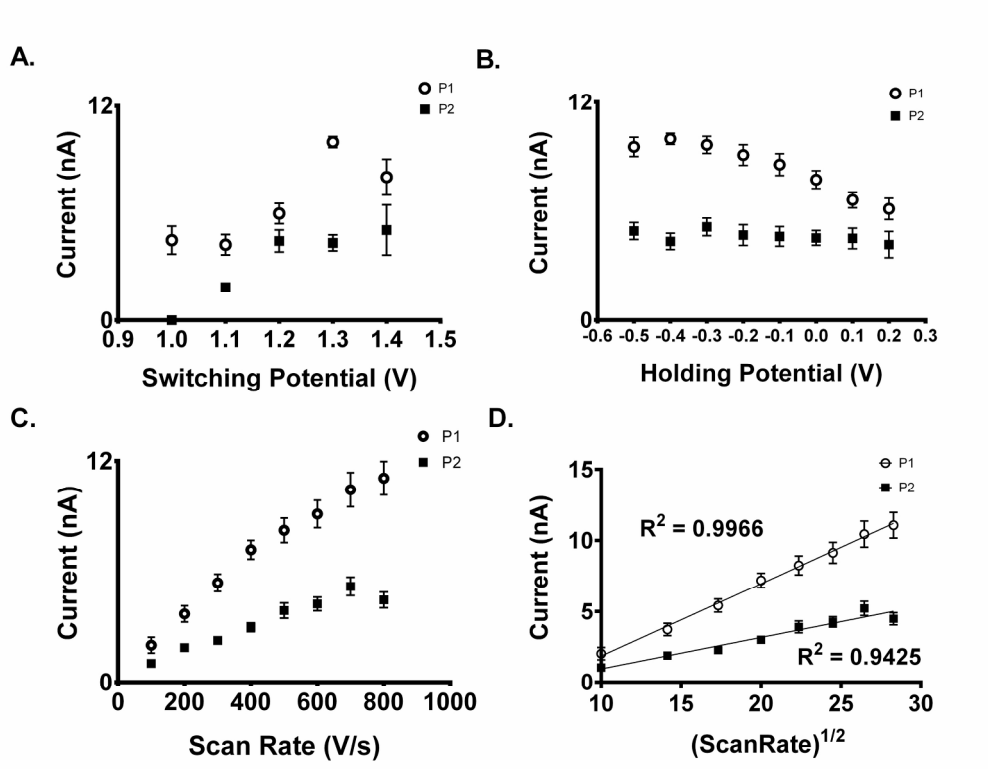

Fig. 6 Optimization of FSCV scanning parameters. (A) Effect of switching potential on oxidation current for the primary peak (circles) and secondary peak (squares) was studied. Switching potential was varied between +1.0 V and +1.4 V while holding potential was held constant at – 0.4 V using a scan rate of 400 V/s. (B) The holding potential was varied from – 0.5 V to + 0.2 V while the switching potential was held at + 1.0 V with a scan rate of 400 V/s. Current responses of peak 1 (circle) and peak 2 (square) at each holding potential were plotted. (C) Dependence of oxidation current of peaks 1 and 2 on scan rate (C) and square root of scan rate (D). The waveform -0.4 V to +1.3 V to -0.4 V was used (for all figures $p<0.001$, n=4, peak one compared to peak two, two-way ANOVA).
212x167mm (300 x 300 DPI)

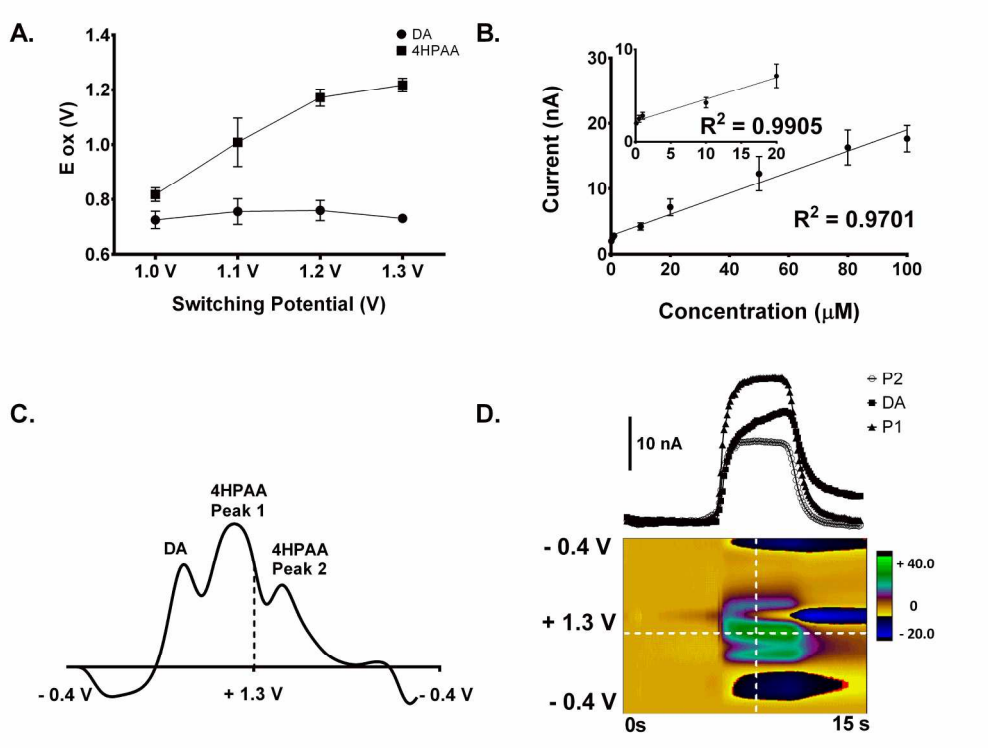

Fig. 7 Cyclic voltammetry of 4HPAA and DA at optimized waveform. (A) Study of oxidation peak potential of 100 μM 4HPAA and 1μM DA. (n=4, p< 0.0001, two-way ANOVA). (B). Concentration study of 4HPAA in the presence of DA. Current responses of the primary oxidation peak was plotted against 4HPAA concentration. (n=3, P=0.0091, t-test) (C) Unfolded CV of 4HPAA and DA. Three oxidation peaks were observed, oxidation peak of DA and 4HPAA (peak 1) were shown on forward sweep and 4HPAA (peak2) on reverse sweep. (D) Color plot (bottom) and current traces of 4HPAA and DA was obtained from the flow injection analysis.
208x157mm (300 x 300 DPI)